

STRENGTH EVALUATION AND MELT RHEOLOGY OF HIGHLY MINERAL FILLED POLYMER COMPOSITES

Winnie Atieno Onyango 

*PhD student, University of Miskolc, Faculty of Materials Science and Engineering
Institute of Energy, Ceramics- and Polymer Technology
3515 Miskolc, Miskolc-Egyetemváros, e-mail: onyango.winnie.atieno@student.uni-miskolc.hu*

Gyorgy Czel 

*university professor, University of Miskolc, Faculty of Materials Science and Engineering
Institute of Energy, Ceramics- and Polymer Technology
3515 Miskolc, Miskolc-Egyetemváros, e-mail: gyorgy.czel@uni-miskolc.hu*

Abstract

This study investigated the effect of high mineral-filled high-density polyethylene (HDPE). The filler as natural zeolite highly affected the mechanical, rheological, and physical properties of the composites. The HDPE composite was extruded up to 60 weight percentage(wt%) to make it possible to use as heat sink material. The electron microscope showed that zeolite has homogeneous distribution inside the composite with zeolite increases even its high filled version. The results showed favorable rheological behavior of the composites that the zeolite has negligible effect on viscosity within the highly filled HDPE. The composites kept the shear thinning behavior in the high shear rate as well. The amount of zeolite filler content improved the mechanical properties of the composites with an increase in the content of the natural filler.

Keywords: *Zeolite -filled composite, Mechanical strength, Melt rheology, mineral zeolite, HDPE*

1. Introduction

The method employed in the processing of composites is based on the selection of matrix materials and reinforcing components. It is common to use minerals as filler materials in the polymer composites. Zeolite composites were made by several authors with a separate need to use a variety of matrices, such as polypropylene (PP) (Kim et al., 2018; Oñate et al., 2023; Belviso et al., 2021; Vaičiukynienė et al., 2024; Laycock et al., 2023; Purnomo et al., 2018) and high-density polyethylene (HDPE) (Purnomo et al., 2016, 2018, n.d., 2020; Khanal et al., 2020; Niang et al., 2018). Polyethylene (PE) (Silva et al., 2020), polylactic acid (PLA) (Oñate et al., 2023; Ayyanar et al., 2023), polyamide (PA) (Bin Matin Saddam & György Czel, n.d.; Lu Zhao et al., 2023) and ultrahigh molecular weight polyethylene (UHMWPE) (Silva et al., 2020; Spiridonov et al., 2020) are also known with zeolite fillers. According to Kajtár et al., high-impact polystyrenes (HIPS1), polycarbonate (PC), poly (methyl methacrylate) (PMMA), polyvinyl chloride (PVC), polystyrene homopolymer (PS), and styrene-acrylonitrile copolymer (SAN) showed that their properties changed widely depending on the weight percentage of the zeolite content (Kajtár et al., 2017). Composite

materials comprise polymers with various chemical compositions and structures and fillers in different structural organizations. Clays, oxides, carbonates are natural and synthetic fillers (Oñate et al., 2023). In case of particle reinforced composites are popular to composed of one or more fiber types in a matrix. Creating composite from polymeric materials requires developing synthesis guidelines for various customized applications. Due to the rising expense of synthetic zeolite fillers and the growing need for environmentally friendly materials, novel composites using natural fillers are being created.

Zeolites have been employed as functional fillers to enhance polymer characteristics. Although, the process technique needs the flow behaviour of the created composite materials, the rheology of polymers loaded with zeolites is not included in published data. One of the main disadvantages of filled composites is that above a certain filler content, the composite material cannot be processed using traditional methods. In the case of these materials, thermal decomposition and mixing of the inhomogeneous filler in the matrix make the production of the product impossible (Macias-Rodriguez, 2024).

Researchers investigate the material’s viscosity at different test temperatures (Macias-Rodriguez, 2024). Rheological characterizations of composites investigated according to other works of literature show changes in the polymer structure resulting from degradation and connect the melting to processability. Only the properties of composites with a maximum zeolite content of 50 wt% have been published based on a literature study (Kajtár et al., 2017). Therefore, the effect of high zeolite loading on the mechanical, physical and rheological properties of polymer composites is still a subject of limited knowledge. Therefore, the main objective of the present research is to determine how the zeolite influenced the mechanical, rheological and physical characteristics of the filled HDPE composites in above 50 % filler content. Present research concentrated on a single polymer system HDPE as a matrix and zeolite particle filler that was prepared by melt extrusion technique from 0 wt% to 60 wt%. The type of filler distribution, the structure of the composite that results from the usage of a twin-screw extruder also the task of the research. In case of rheological investigations, Begley correction provides an apparent viscosity value to obtain a genuine shear stress and true viscosity.

2. Experimental

2.1. Raw materials and composite preparation methods

Table 1. Typical properties of HDPE and natural zeolite material

Material	Tensile modulus, MPa	Strain at the yield, %	Melt flow rate (MFR), g/min	Melt Temp, °C	Density, kg/m ³	Hardness, +23°C, kJ/m ²	Water absorption, %	Compressive strength, MPa
HDPE	1650	11	0.3	125-135	958	65 ^a	0.001-0.015	-
Natural zeolite	-	-	-	1 340	1990	4-6.5 ^b	34 - 36	33

^a Shore D hardness scale R, ^b Mohs scale

For our experiments, TIPELIN 6000 B HDPE from MOL Ltd in Tiszaújváros, Hungary, was used as the polymer matrix. Table 1. shows the typical properties of HDPE and zeolite.

The natural Zeolite as crystalline aluminium-hydro-silicates was obtained from Geo-product Ltd. Mád Tokaj. with the sizes 1 µm -110 µm with most of the highest at (87.29%) of 45 µm sizes. The evaluated density was 1990 kg/m³.

Before manufacture, the zeolite was dried in a PIOVAN DP604 vacuum drier for 48 hours at 120 ± 2°C, resulting in a 0-1% moisture content based on the zeolite's oven-dry weight. The PRISM TSE 16TC twin screw extruder was used for melt mixing after the zeolite powder had been dried in the drying chamber. HDPE and zeolite filler in varying concentrations and sizes were homogeneously blended with the twin screw extruder.

The composites were fed to the KRAUSS MAFFEI KM80-160C1 injection moulding machine after being ground into granules with a PIVION RSP15/15 blade grinder. The test samples were prepared and test using ASTM D 638 test standard. Pure HDPE was used to prepare the reference sample similarly. Table 2. shows the composite formulation. The process's flow chart is displayed in Figure 1. The composite preparation method is in table 3.

Table 2. Composite compositions and number of robes

Codification	Composition		
	Zeolite (wt%)	HDPE (wt%)	Number of pieces
HDZ00I	0	100	20
HDZ03I	15	85	20
HDZ04I	20	80	20
HDZ05I	40	60	20
HDZ06I	60	40	20
TOTAL NUMBER OF SAMPLE PIECES			100

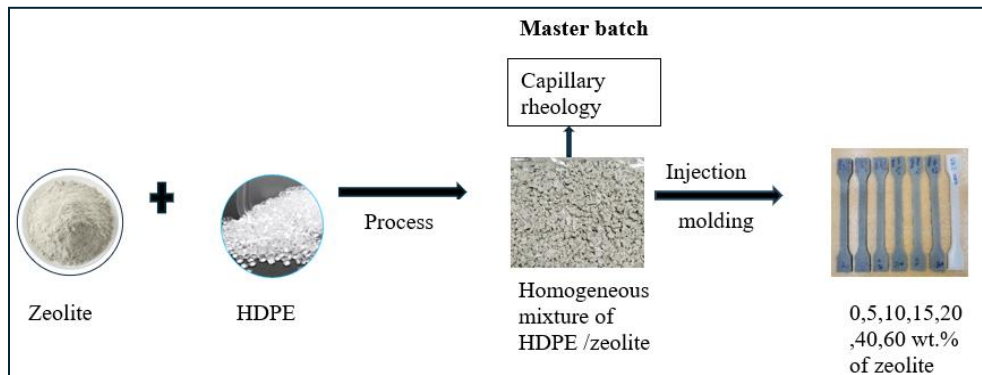


Figure 1. Representation of HDPE/zeolite composite preparation steps

Table 3. Composite preparation and applied tests

zeolite content	sample code	Drying	Twin Screw Extrusion	Injection Molding	Shore D Test	Charpy Impact Test	Tensile Test.	SEM	Rheology
0%	HDZ00	X	X	X					X
	HDZ00I				X	X	X	X	
15%	HDZ03	X	X	X					X
	HDZ03I				X	X	X	X	
20%	HDZ04	X	X	X					X
	HDZ04I				X	X	X	X	
40%	HDZ05	X	X	X					X
	HDZ05I				X	X	X	X	
60%	HDZ06	X	X	X					X
	HDZ06I				X	X	X	X	

Figures 2(a) and (b) show the distribution of zeolite size and the drying curve. We computed the average drying percentage using equation (1)

We computed the average drying percentage using equation (1). (b)

$$U\% = \frac{\Delta M}{M_0} \cdot 100\% \tag{1}$$

Where U is the average drying percentage, ΔM is the change in mass of zeolite and M₀ is the initial mass of zeolite before drying.

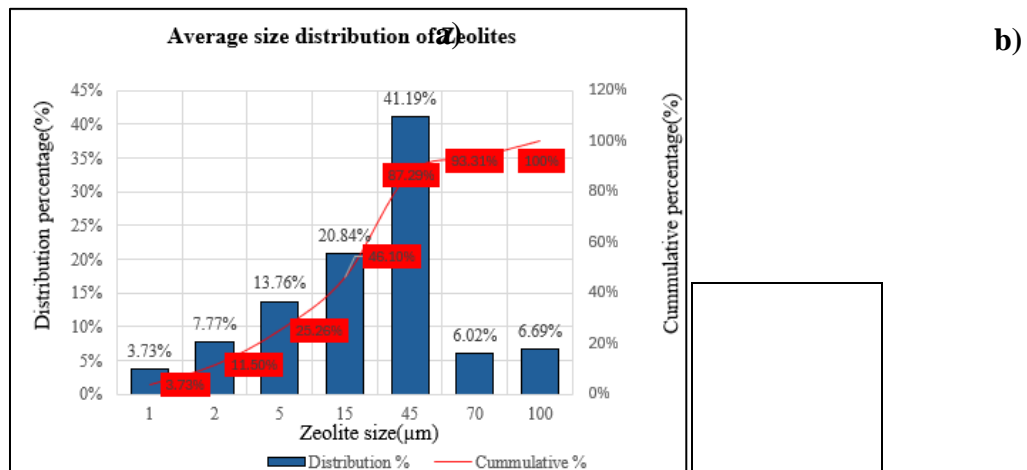


Figure 2. Zeolite size distribution **a)** (Bin Matin Saddam & György Czel, n.d.) and Zeolite drying curve **b)**

Weight Fraction (wt%) was calculated using equation (2). Where m_f is the mass of the filler and m_m is the weight of the Matrix.

$$\text{wt}\% = \frac{m_f}{m_f+m_m} \cdot 100\% \quad (2)$$

Twin screw extruder parameters were: barrel zone=190 °C, Zone1=195 °C Zone2=220 °C, Zone3=235 °C, die section=230 °C. The specimens are injection molded by utilizing a Krauss Maffei KM65-160C1 injection molding machine. The molding conditions of the sample parameters are given in Table 4.

Table 4. Moulding process parameters

Injection Pressure	75bars
Holding pressure	850 bars
Screw rotation speed	200 rpm
Cooling time	15 seconds
Temperatures of heating zones (from hopper section)	120 °C, 200 °C, 240 °C, 254 °C, 260 °C
Mold temperature	35 °C,
Hopper section temperature	50 °C,

2.2. Morphological Characterisation of the Composites

The micrographs of the powders and the cryogenically fractured surfaces of the composites were examined using SEM Zeiss EVO 10 (Carl Zeiss Microscopy) with an accelerating voltage of 10 kV. Before imaging, the probe surfaces were coated with gold by using an ionisation chamber. The generated samples were subjected to an electronic microscope for microscopic analysis to observe the distribution of zeolite particles inside the composite, and the HDPE-zeolite interface and dispersion within the composite. A small broken polymer sample from the impact test analysis was gathered, cleared, and cleaned before being meticulously examined at magnifications of 100 under an electron microscope.

The HDPE comprises carbon (see Figure 3a) and hydrogen atoms. The hydrogen atoms are not indicated since the lower elements are not detected in the Energy Dispersive Spectrometer (EDS). The zeolite contains a very high percentage of silicon, followed by aluminium, some potassium, and oxygen. The EDS analysis verify the zeolite atomic content as hydro-silicate. The natural zeolite is a crystalline aluminium-hydro-silicate containing Al, Si, K, Ca and O (Fig.3b).

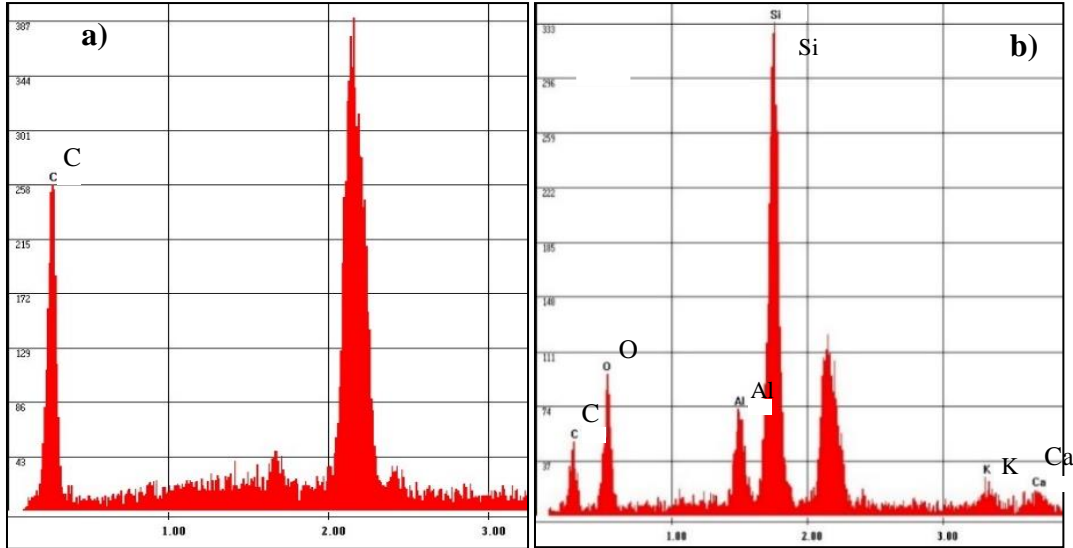


Figure 3. The Energy Dispersive Spectroscopy (EDS) analysis of-HDPE **a)** and zeolite **b)**

2.3. Mechanical tests

Tensile tests were done to evaluate the moduli and the tensile strength of the new composite materials. The universal tensile test machine INSTRON 5566-J9154 was used to conduct the tensile following the ASTM D 638 standard of measurement. The configuration of the specimen was a dog bone shaped 3.0 mm thick with a length of 80 mm and a width of 4 mm. A tensile testing machine was employed to subject the specimen to axial elongation. The resultant loads on the specimens at fracture. The modulus was calculated according to equation 3.

$$E = \frac{\sigma_2 - \sigma_1}{\varepsilon_2 - \varepsilon_1} \quad (3)$$

Where E is the Young modulus, σ_1 and σ_2 are the stresses at $\varepsilon_2=0.3\%$ and $\varepsilon_1=0\%$ strain points. Tests were executed at room temperature (25°C), and the presented results are an average of 5 experiments.

Impact tests were done to evaluate the zeolite cause brittleness of the new materials. According to the ISO 179 standard method of measurement, the degree of resistance of the formed polymers to impact loading using the Charpy impact testing method using INSTRON CEAST 9050 type 7615. On the specimens, a 5 Joules load at a speed of 5.24 m/s, allowing the different energy values to disperse before fractures were applied. Every sample was 8 mm by 4 mm in thickness. The specimen is placed on the base plate with the v-notch centered. The potential energy at 150° less the energy remaining after impact strength, which is the energy absorbed by the broken test specimen. Each batch had 5 probes per test.

The Shore D hardness specimen was prepared according to the ASTM D2240 standard using a Zwick /Roell 2961 machine. The Shore D hardness was compared according to the average calculated values of 5 probes per test per batch.

2.4 Melt rheology of zeolite-filled HDPE polymer

Newtonian fluids have a viscosity that is independent of shear rate. In this case a single viscosity measurement is required. Pseudoplastic non-Newtonian behaviour of fluids is typically seen in thermoplastic polymer melts or polymer composites in melt state. When the shear rate increases, viscosity decreases, the melted materials show shear thinning behaviour. This can be advantageous for a variation of products processed by injection molding. The shear rate changes dramatically under high shear stress.

The melt flow index (MFI) is related to the viscosity of the melt, but it only gives a single-point measurement, which is suitable if the applied shear rate is the same throughout the entire use of the product process. However, this rarely happens. Much more information about the flow behavior of raw materials can be obtained if the entire flow curve, or at least the deformation speed range typical for injection molding is made visible. In the production of polymer composite parts by injection molding, the section of the entire flow curve is at least between 500 -50000 s⁻¹ essential in the shear rate section. In practice, this means that the entire flow curve must be recorded. Capillary rheometry and its experimental equipment provide the possibility of recording the total flow curve in the simplest way. To perform extrusion capillary rheometry, apart from the equipment, theoretical relationships are also needed. The equations allow the numerical representation of viscosity. The change in viscosity can thus be displayed as a function of shear stress. The basic parameters of capillary rheometry are the geometric size of the capillary, the value of the head pressure of the extruder and the mass flow passing through the capillary. To calculate the shear stress, it is necessary to know the torque of the screw. The following formulas were used during the rheology process our rheology evaluation.

The apparent shear rate ($\dot{\gamma}_{app}$) for round capillary die is calculated by using Eq. (4).

$$\dot{\gamma}_{app} = \frac{4\dot{Q}}{\pi R^3} \quad (4)$$

Where \dot{Q} is the volumetric flow rate, R is the radius of the capillary in our case R= 1 mm.

The flow rate was determined by the measured mass flow (5). Where ρ is the melt density of the composite.

$$\dot{m} = \rho \dot{Q} \quad (5)$$

The apparent shear is calculated as:

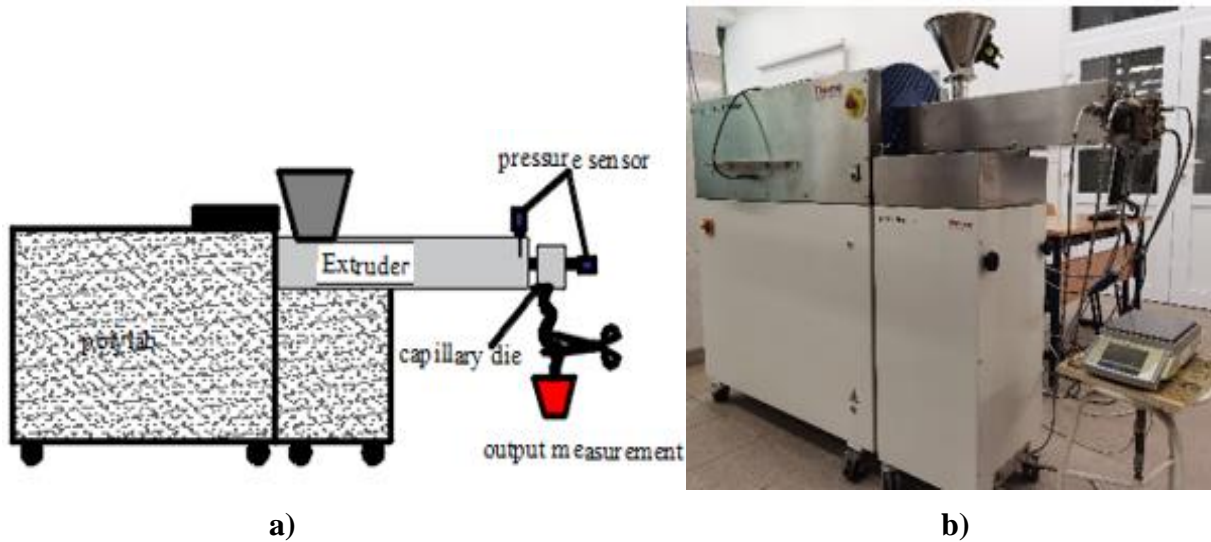
$$\tau_{app} = \frac{R p}{2L} \quad (6)$$

Where R is the capillary radius, p is the pressure and L is the capillary length. The uncorrected apparent viscosity (η_{app}) was calculated as:

$$\eta_{app} = \frac{d\tau}{d\dot{\gamma}} \quad (7)$$

Pressure-driven melt rheology measurements were performed on a Thermo-HAAKE polylab rheometer equipped type Typ557-9320 with an extruder device of model Tzp557-2804 at 235-250 °C, using a parallel capillary die with a diameter of 2 mm with L/D of 10 mm for zeolite filled composites. The specimens used

were extruded at an initial rotation speed of 5 rpm with the end value of 60 rpm at 5 steps of speed to give various speeds of composite flow see in fig 4b).



a) *Figure 4. Capillary rheology theoretical set up a) and Thermo Haake 557-9320 rheometer b)*

3. Results and Discussion

3.1. Microstructural analysis

Observing the crushed surface area of the composites (Fig.5), the zeolite distribution is uniform throughout the polymer matrix (see Fig.5/b-d). Figure 5/b-d shows the well-embedded situation of the zeolite particles even in a high zeolite filler content. Fig5b shows a zeolite grain (marked with a circle) that prevented the crack from propagating, and the crack changed direction. As the amount of zeolite increases, the cracks run at the boundary between the zeolite and the matrix (see Fi.5c, d).

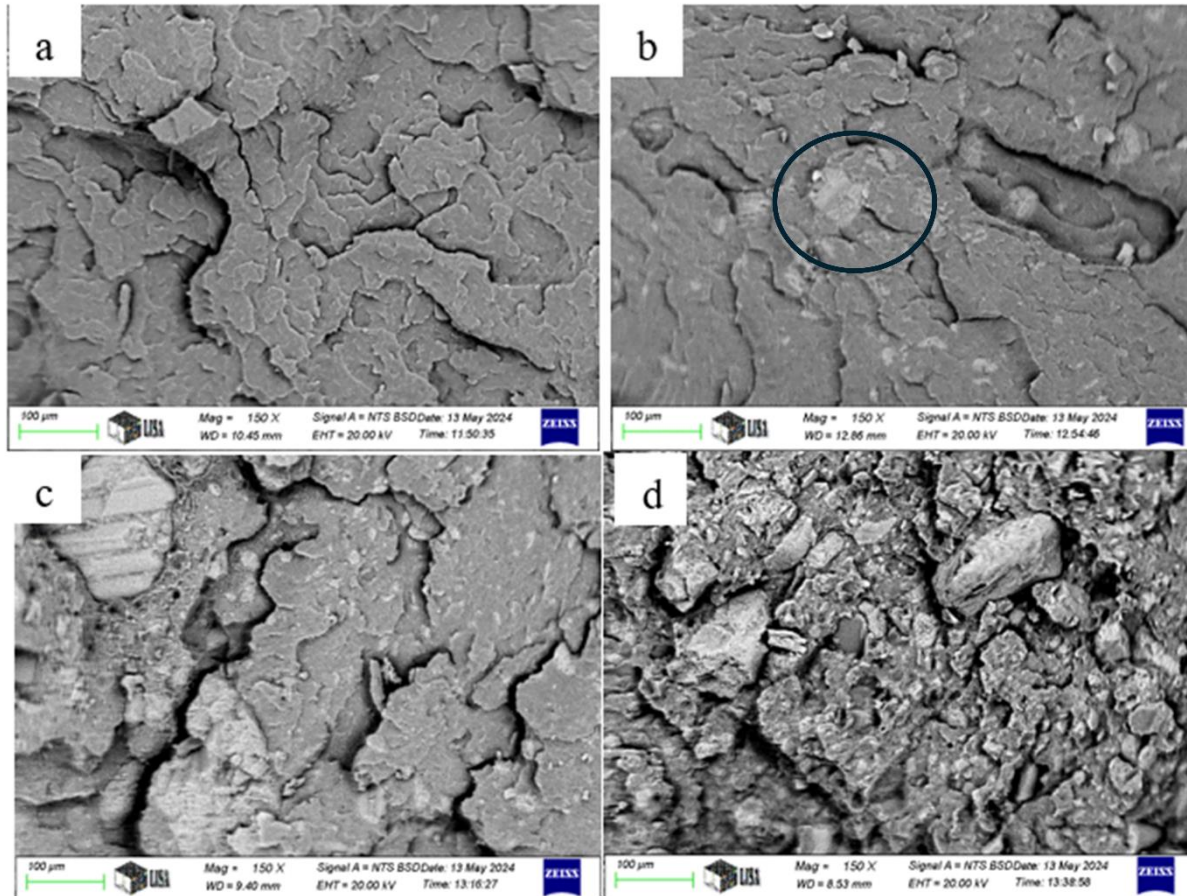


Figure 5. Scanning electron microscopic micrographs of zeolite-filled HDPE. a) 0 wt%, b) 15 wt%, c) 20 wt%, d) 40 wt% zeolite

The SEM photos in Figure 6c) show signs of a shattered zeolite, clearly demonstrating this. Figure 6c) shows the fracture did not proceed at the interface of the matrix and the zeolite grain, but that the zeolite particle fractured. Therefore, the high magnification SEM pictures show a notable wetting and encapsulating of Zeolite by the HDPE, visually verifying the interfacial interactions. This may result from hydrogen bonds forming between these terminal silicate groups and the carboxylic groups of the HDPE when thermal decomposition occurs around the zeolite boundary. As it is visible here, the physio-mechanical properties of any composite material are largely determined by the filler–matrix interfacial interactions.

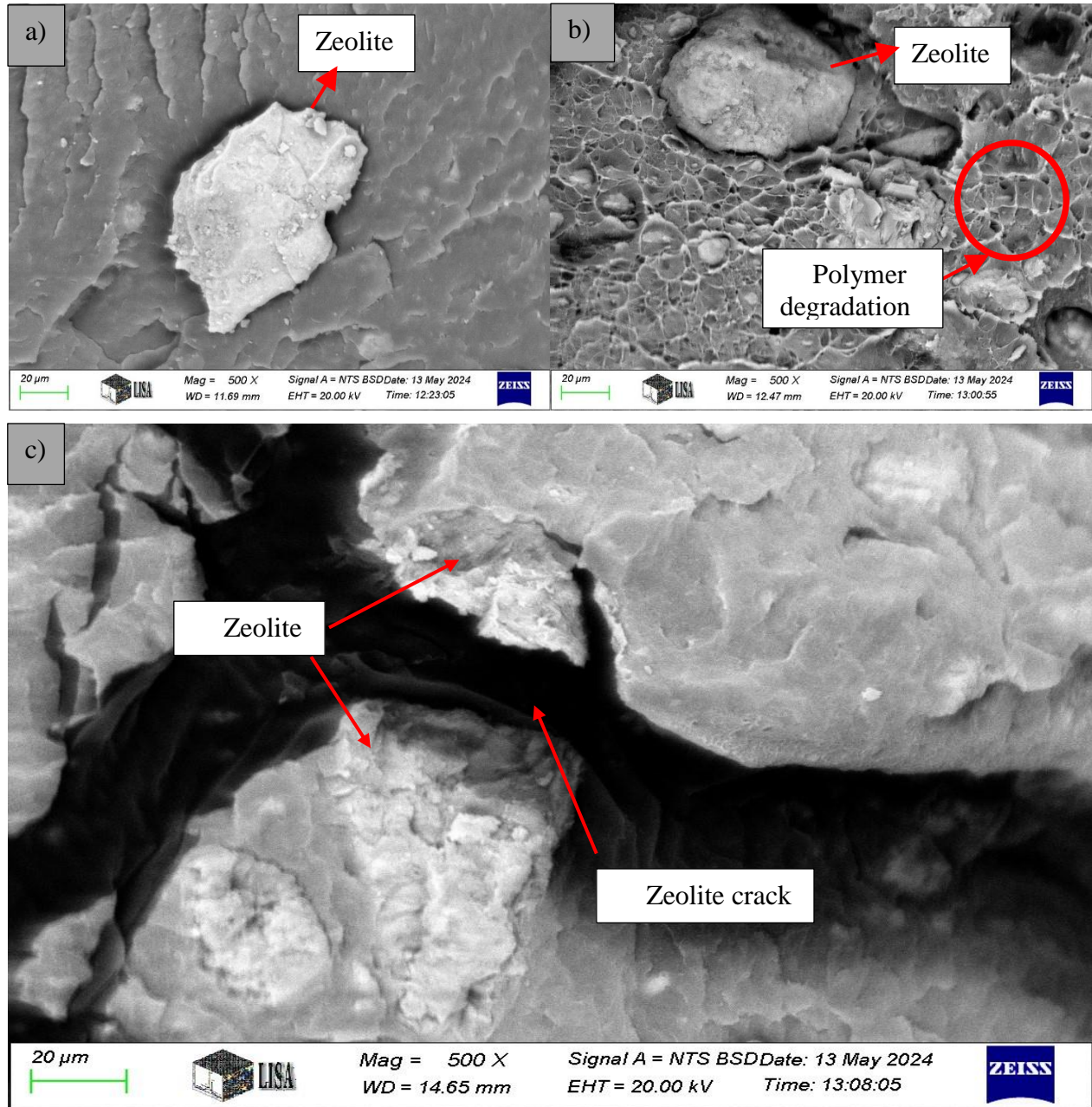


Figure 6. Interaction of HDPE-zeolite boundary

3.2. Tensile test

In the case of the composites, tension transferring is a complex process between the matrix and filler. Stress-strain curves show big difference especially in elongation compare the virgin HDPE and the zeolite filled composites. The tensile test results are shown in Figures 7 and 8. A slight tensile strength increase was observed upon zeolite addition in case of 60 wt% zeolite content. According to research by Purnomo et al (Purnomo et al., 2016), the increase in tensile strength is caused by a rise in covalent and hydrogen bonds with the OH group and the oxygen of each group carboxyl adds a connection between the filler and the matrix the same could be observed.

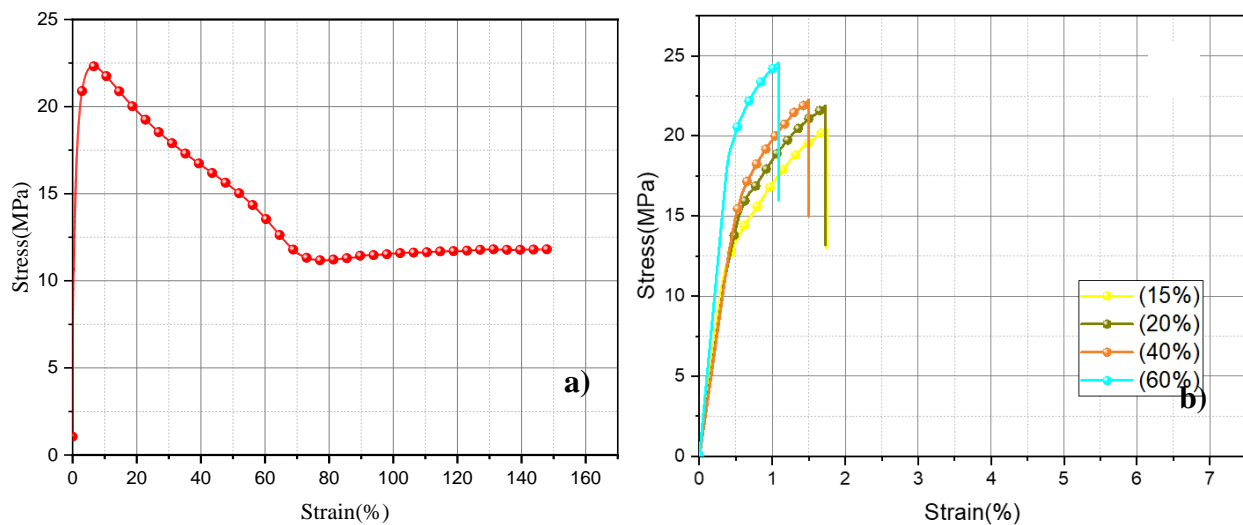


Figure 7. Tensile curve for pure HDPE **a)** and Tensile curves of zeolite-filled HDPE composites **b)**

The highly filled composite at 60 wt% had the highest tensile strength of a 15.8% increase. Figures 8a) and 8b) display the tensile stress at 0.3 strain and Young's modulus for HDPE composites containing 0 wt%, 15 wt%, 20 wt%, 40 wt%, and 60 wt% zeolite. Tensile modulus tends to rise with increasing zeolite concentration in HDPE composites reaching 4441 MPa in the case of 60 wt% zeolite. This is most likely caused by the addition of a rigid filler (zeolite) to a flexible material (HDPE), which tends to increase the product's overall rigidity and impede the free movement of HDPE chains.

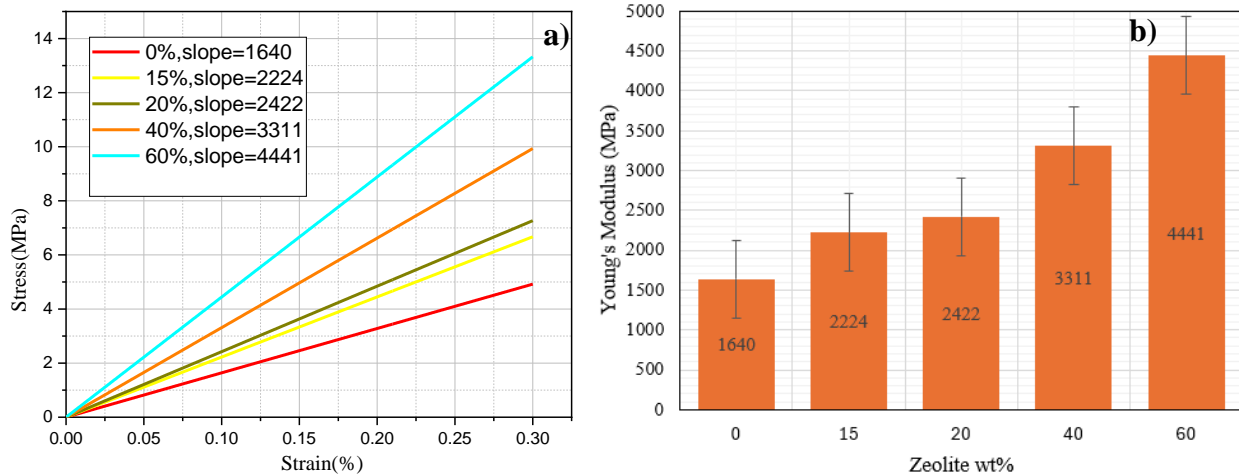


Figure 8. Comparison of HDPE/zeolite composite stress at 0.3% strain a) and Young's modulus b)

3.3. Impact test and Shore D hardness test

Charpy's impact strength changing as a function of wt% is plotted in Figure 9a) It takes less energy to break as the zeolite content rises. Impact strength decreases with an increase in zeolite content. As the filler content increased, the new composites became brittle, and HDPE lost its ability to be easily plasticized. The overall decline of Charpy's impact strength is 29.5%.

According to the Shore D results in Figure 9b), the sample with 60 wt% zeolite content is the hardest composite. The difference in hardness between virgin HDPE and HDPE filled with 60% by weight is significant.

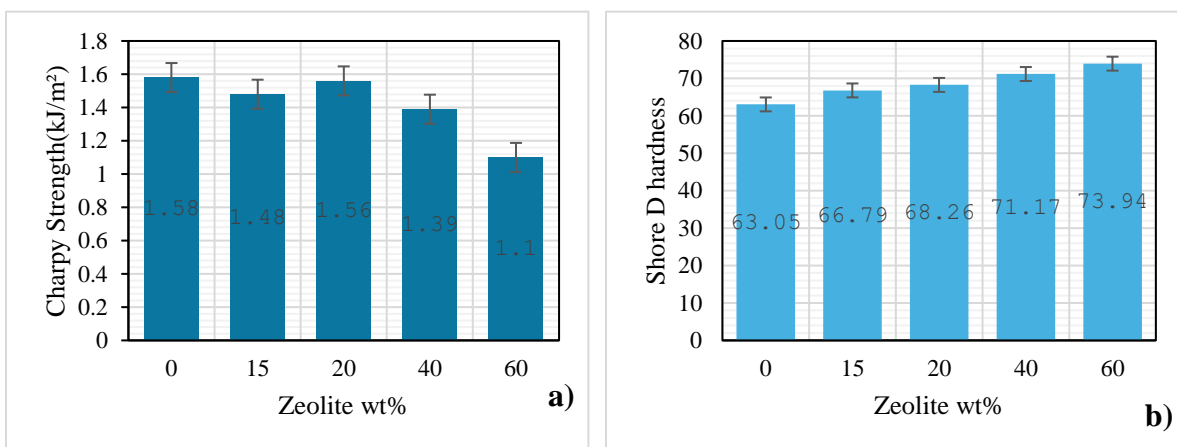


Figure 9. a) Charpy Impact strength of HDPE-zeolite composite. b) Shore D hardness with weight fraction of zeolite.

3.4. Rheological results

The pressure fluctuation in the rheometer is less than 1% at all shear rates. These pressure fluctuations are typically more pronounced in composites with high filler levels but should be kept low. The pressure fluctuation depends on the size of the particles and the amount of filler. The temperature rise caused by dissipation is one of the often-neglected effects during capillary measurements, but it can be significant for polymeric materials with a high degree of filling. In our experiments, we took special care to keep the fluctuation of the tool temperature as low as possible. The temperature was selected and set in the control unit in a typical high-pressure capillary rheometer measurement setup. Consequently, the calculated viscosity curve received the set temperature value.

There are two temperature transducers in our investigation. At the extruder barrel TM-D₂ and the other at the die head TM-D₁. However, there is some heat dissipation. Since the stiff filler is essentially just "swimming" with the flow of the polymer, almost all the heat dissipated in our case of stiff fillers is created in the matrix (Figure 11.) raising the matrix temperature. Due to the poor heat conductivity of the polymer matrix, the heat that dissipates will remain in the polymer at shear rates more than 100 s⁻¹, raising the polymer's temperature while simultaneously lowering its viscosity as it is well visible in the Fig 11. where step by step rising

TM-D₁ curve is visible, but the temperature deviation not higher than 5°C. The actual temperature corresponding to a given viscosity value is higher than the temperature typically used, as shown in Figure 10. Velocity steps are crucial in the calculation of viscosity, since each velocity plateau results in another point of the entire rheological curve. The speed and thus the required pressing torque also increases, and the amount of material passed through the capillary also increases step by step. The shear rate (τ) changes with the change in the screw speed, while the change in viscosity can be inferred by measuring the pressure and mass flow using the Hagen-Poiseuille relation.

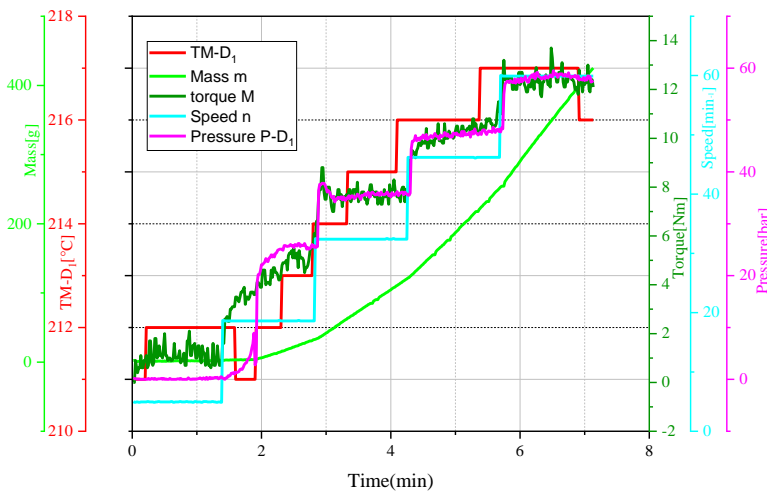


Figure 10. Measured rheological raw data of 20 Wt% Zeolite filled HDPE

In Figure 11. the introduction of zeolite increased the temperature from 212-217 in the die head. This fact directly influences the mass rate as shown in Figure 11a). On the other hand, the gradually changing rotation speed of 5-60 rpm indicates an increasing demand for torque, which is largely due to the amount of ceramic fillers. The maximum required torques of 15 wt%, 20 wt% and 40 wt% filled composites are 12.5, 14 and 15 Nm, respectively, as can be clearly seen in Figure 11b). At a higher torque, the amount of material transported in each time is greater, which naturally results in an increase in pressure at the inlet of the capillary. These torque values increase with increasing zeolite content up to 40% by weight for the same delivery power (\dot{Q}) see in Fig 11b). The reason for this is that with a higher zeolite content, it is more difficult to shear the composite melt, a higher torque and thus a higher shearing energy is required. Intense shear results in higher temperatures, resulting in lower viscosity favourably.

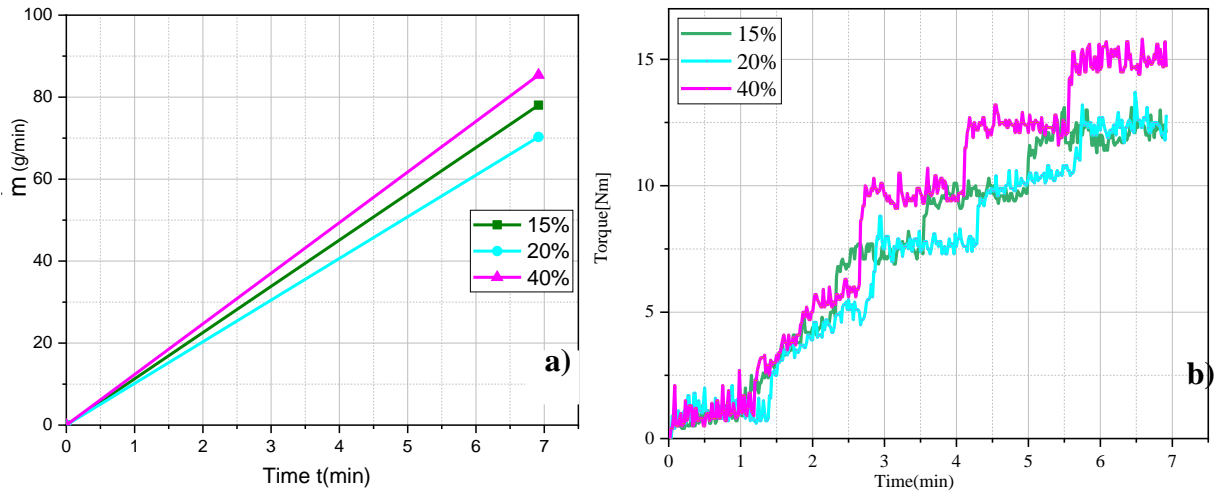


Figure 11. Effect of the zeolite amount on the mass rate **a)** and torque **b)**

In the range of applied shear rates, the HDPE-zeolite composites showed non-Newtonian, i.e. pseudoplastic, behavior (Figure 12). In this reference test, the shear rate range was the same as that commonly used in extrusion processing. Shear thinning, or a decrease in viscosity with increasing shear rate, is a characteristic of molten polymers.

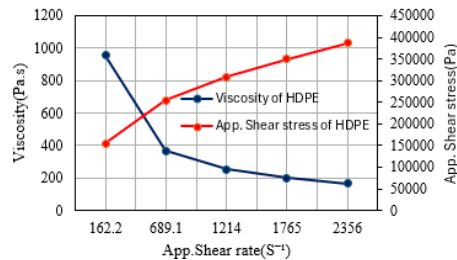


Figure 12. Flow and viscosity curve of virgin HDPE

Figure 13. shows that the viscosity curves of zeolite-filled HDPE are comparable to the viscosity curves of virgin HDPE as it was shown in Figure 12. The viscosity curve of highly filled composites has almost the same curve run. The higher the filler content, the lower the viscosity of the composite. Due to the structure of the zeolite, the change is not high. The highly filled zeolite composite also shows a high degree of shear thinning, as can be seen in Figure 13.

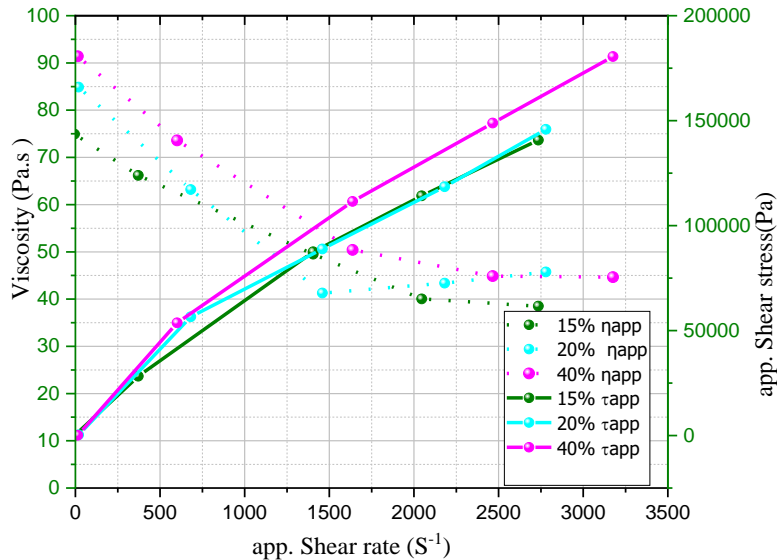


Figure 13. Effect of zeolite on the uncorrected flow curve and viscosity

The addition of fillers results in a large reduction in melt viscosity. It also occurs at lower shear rates (75 Pas, 85 Pas and 92 Pas at 15 wt%, 20 wt% and 40 wt% of zeolite) due to interparticle interactions within the zeolite compared to the unfilled polymer melt. At low shear rates, the filled polymers are viscous and show a large viscosity change with increasing filler concentration, see the beginning of the curves in Figure 13. However, the effect of the filler on the viscosity decreases in the range of higher deformation rates.

4. Conclusions

This work investigated the effect of natural zeolite added to the HDPE matrix at 0 wt%, 15 wt%, 20 wt%, 40 wt% and 60 wt%. Based on the mechanical, rheological and microstructural properties analysis, a high-performance composite can be made using only zeolite and HDPE, without additional additives, by extrusion (melt processing) and injection moulding. HDPE composites filled with zeolite produced good strength material properties. A good interfacial adhesion between the HDPE matrix and the natural zeolite filler can be demonstrated. This is confirmed by the SEM microstructure analysis. Precursors of rheological results for analysis of viscosity change in HDPE-zeolite composites. With melt forming, even HDPE matrix composites with a high degree of filling can be processed and are suitable for the application of injection

molding technology. These composites are more environmentally friendly and do not rely on the declining availability of fossil fuels.

5. Acknowledgments

The research work described in the article is part of the CIRCLETECH 101079354 project " Circular Manufacturing_ " – within the framework of the European Union's Horizon European Program by the European Social Fund. The financial assistance of the Polymer Laboratory at Miskolc University towards this research is hereby acknowledged.

References

- [1] Kim, D., Thanakkasaranee, S., Seo, J., & Khan, S. B. (2018). Effect of porous zeolite on temperature-dependent physical properties of polypropylene/octadecane (PP/OD) composite films. *Express Polymer Letters*, 12(7), 658–674. <https://doi.org/10.3144/expresspolymlett.2018.56>
- [2] Oñate, A., Sáez-Llanos, T., Jaramillo, A., Vargas-Silva, G., Meléndrez, M., & Medina, C. (2023). Enhancing mechanical properties of PLA and PP composites through ionic zeolite with copper nanoparticle reinforcement: microstructural and micromechanical characterization. *International Journal of Advanced Manufacturing Technology*, 129(7-8), 3375–3386. <https://doi.org/10.1007/s00170-023-12499-3>
- [3] Belviso, C., Montano, P., Lettino, A., Toschi, F., Lambertini, V. G., Veca, A. D., Moschetto, E., Cavalcante, F., & Guarnaccio, A. (2021). Determining the role of the method used to recycle polypropylene waste materials from automotive industry using sepiolite and zeolite fillers. *Journal of Material Cycles and Waste Management*, 23(3), 965–975. <https://doi.org/10.1007/S10163-021-01184-W>
- [4] Vaičiukynienė, D., Kantautas, A., Nizevičienė, D., Vaičiukynas, V., & Alaburdaitė, R. (2024). Utilization of polypropylene waste and zeolitic by-product in composite materials. *Materials Letters*, 136563. <https://doi.org/10.1016/j.matlet.2024.136563>
- [5] Laycock, B., Pratt, S., & Halley, P. (2023). A perspective on biodegradable polymer biocomposites - from processing to degradation. *Functional Composite Materials*, 4(1). <https://doi.org/10.1186/s42252-023-00048-w>
- [6] Purnomo, P., Subri, M., & Setyarini, P. (2018). Fracture development and deformation behavior of zeolite-filled high density polyethylene annealed composites in the plane stress fracture. *FME Transactions*, 46(2), 165–170. <https://doi.org/10.5937/fmet1802157z>
- [7] Purnomo, P., Soenoko, R., Suprpto, A., & Irawan, Y. S. (2016). Impact fracture toughness evaluation by essential work of fracture method in high density polyethylene filled with zeolite. *FME Transactions*, 44(2), 180–186. <https://doi.org/10.5937/fmet1602180P>
- [8] Purnomo, P., Setyarini, P. H., & Anggono, A. D. (2020). Fiber orientation effect on fracture toughness of silk fiber-reinforced zeolite/HDPE composites. *FME Transactions*, 49(1), 128–134. <https://doi.org/10.5937/fme2101128P>
- [9] Purnomo, P., Subri, M., & Subri, M. (n.d.). *Tensile behavior of zeolite-filled high density polyethylene annealed composite*. www.iscogi.unwahas.ac.id

- [10] Khanal, S., Lu, Y., Ahmed, S., Ali, M., & Xu, S. (2020). Synergistic effect of zeolite 4A on thermal, mechanical and flame-retardant properties of intumescent flame retardant HDPE composites. *Polymer Testing*, 81. <https://doi.org/10.1016/j.polymertesting.2019.106177>
- [11] Niang, B., Ly, E. H. B., Diallo, A. K., Schiavone, N., Askanian, H., Verney, V., Badji, A. M., Diakite, M. K., & Ndiayne, D. (2018). Study of the thermal, rheological, morphological and mechanical properties of biocomposites based on rod-of typha/HDPE made up of typha stem and HDPE. *Advances in Materials Physics and Chemistry*, 8(9). <https://doi.org/10.4236/ampc.2018.89023>
- [12] Silva, B. J. B., Melo, A. C. S., Silva, D. S., Sousa, L. V., Quintela, P. H. L., Alencar, S. L., & Silva, A. O. S. (2020). Thermo-catalytic degradation of PE and UHMWPE over zeolites with different pore systems and textural properties. *Ceramica*, 66(380), 379–385. <https://doi.org/10.1590/0366-69132020663802948>
- [13] Ayyanar, C. B., Marimuthu, K., Sridhar, N., Mugilan, T., Alqarni, S. A., Katowah, D. F., Sanjay, M. R., & Siengchin, S. (2023). Mechanical and materialistic characterization of poly lactic acid/zeolite/hydroxyapatite composites. *Journal of Inorganic and Organometallic Polymers and Materials*, 33(9), 2743–2751. <https://doi.org/10.1007/s10904-023-02647-3>
- [14] Bin Matin Saddam, & György Czél. (n.d.). *Heat conductive polymers and their behavior concerning their tribological aspects*.
- [15] Zhao, L., Chen, J., Pan, D., & Hou, Y. (2023). Robust, fire-retardant, and water-resistant wood/polyimide composite aerogels with a hierarchical pore structure for thermal insulation. *Gels*, 9(6), 467. <https://doi.org/10.3390/gels9060467>
- [16] van Heemst, J. J., Zant, E., Schennink, G. G. J., Rodenburg, J. A., Rodenburg, J., Rodenburg, T.: *Starch-based biodegradable polymer; Method of manufacture and articles thereof*, European Patent, EP 2 493 975 B1, published 2017.03.29.
- [17] Spiridonov, A. M., Sokolova, M. D., & Okhlopkova, A. A. (2020). Polymer composite materials based on ultra-high-molecular-weight polyethylene filled with organomodified zeolite. *Polymer Science - Series D*, 13(3), 311–314. <https://doi.org/10.1134/S1995421220030181>
- [18] Kajtár, D. A., Kenyó, C., Renner, K., Móczó, J., Fekete, E., Kröhnke, C., & Pukánszky, B. (2017). Interfacial interactions and reinforcement in thermoplastics/zeolite composites. *Composites Part B: Engineering*, 114, 386–394. <https://doi.org/https://doi.org/10.1016/j.compositesb.2016.12.015>
- [19] Macias-Rodriguez, B. (2024). Rheology-based techniques. In C. Palla & F. Valoppi (Eds.), *Advances in Oleogel Development, Characterization, and Nutritional Aspects* (pp. 471–496). Springer International Publishing. https://doi.org/10.1007/978-3-031-46831-5_19

Symbols and notations

PA	polyamide
SEM	Scanning Electron Microscope
TGA	Thermogravimetric analysis
WPC	Wood polymer composite
HDPE	High Density Polyethylene

PC	Polycarbonate
PE	Polyethylene
PP	Polypropylene
PLA	Poly lactic acid
PMMA	Poly (methyl methacrylate)
PVC	Polyvinyl chloride
PS	Polystyrene homopolymer
SAN	Styrene-acrylonitrile copolymer
UV	Ultraviolet
MFI	Met flow index.
M _o	Original mass
MVR	Melt Volume Rate,
WF	Weight fraction (wt%)
VOC	volatile organic compounds
WCAs	water contact angles
PU	polyurethane
3D	three-dimensional
XRD	X-ray diffraction
FT-IR	Fourier transform-infrared spectrometer
SEM	Scanning electron microscope.
EPS	Expanded polystyrene.
MAH	Maleic Anhydride
FA	Fly ash
BM	Base material
MAPP	Maleic anhydride-modified polypropylene
HIPS	High impact polystyrene copolymers.
DINP	Diisononyl phthalate
ZN	Natural zeolite
AZ	Ammonium zeolite
THEIC	Tris (2-hydroxyethyl) isocynurate
APP	Ammonium polyphosphate
UHMWPE	Ultrahigh molecular weight polyethylene
MAP	Mono ammonium phosphate.
MCC	microcrystalline cellulose
FRs	fire retardants
TS	thickness swelling
DSC	Differential Scanning Calorimetry
TGA	Thermogravimetric Analysis
SF	silk fibre
SE	standard error
EDS	Energy dispersive spectrometer